29th Congress of the International Council of the Aeronautical Sciences
St. Petersburg, Russia; September 7-12, 2014

INTRODUCING RESIDUAL STRESSES IN THIN ALUMINIUM STRUCTURES BY LASER GENERATED TEMPERATURE FIELDS

A. Groth*, N. Kashaev*, N. Huber*
***Helmholtz-Zentrum Geesthacht, Institute of Materials Research, Materials Mechanics / ACE-Centre, Max-Planck-Straße 1, D-21502 Geesthacht, Germany**

Keywords: *Laser heating, aluminium alloy, residual stresses, fatigue crack growth*

Abstract

Since the development of high power laser sources, laser heating was investigated as a tool to retard fatigue life time. This is especially important for aircraft aluminium alloys to safe weight and costs. In previous works, laser heating was demonstrated as a method to retard fatigue crack growth. In order to determine the residual stress field a combined heat flux and mechanical finite element simulation followed by a fracture mechanics simulation was found to be a suitable method to assess the improvement of the fatigue crack growth behaviour.

In this work the approach is transferred from small scale laboratory C(T)100 specimens of aluminium alloy 2198 with a thickness of 5 mm to larger M(T)200 specimens of the conventional aerospace aluminium alloy 2024 with a thickness of 2 mm. For the modified specimen geometry, thickness, and material a new experimental setup was constructed. Laser heating with two different sets of parameters was applied to generate the analysed samples. The influence of laser heating on the material properties is characterised by hardness measurements and optical microscopy. Additionally, the introduced residual stresses are determined by x-ray synchrotron diffraction. Eventually, the lifetime is compared to that of the base material by fatigue crack growth tests.

1 Introduction

Welding processes exhibit a high potential to save costs and weight in the production of modern lightweight structures. During the production of these structural components mechanical and thermal processes induce residual stresses which take influence on the development of fatigue cracks during the lifetime of the different components. Especially in welded integral structures, fatigue crack growth has to be taken into consideration, because a propagating crack can cause severe damage to the structure by penetration into the welded stiffener [1].

As a possible method to improve the residual stress state of such components, local laser heating was applied by Schnubel et. al. [2, 3]. Laser heating introduces residual stresses in welding direction. In the direction of the heating line tensile residual stresses are generated which are compensated in the vicinity of the heating line by corresponding compressive residual stresses. These compressive stresses are expected to retard the fatigue crack growth and increase for this reason the fatigue lifetime.

The positive effect of laser heating on the fatigue crack growth retardation was demonstrated on coupon scale C(T)100 specimens of AA2198 T8 with a thickness of 5 mm. It was shown, that the lifetime of such C(T)100 specimen can be extended by more than 100 % [2]. This increase of the fatigue lifetime also was predicted numerically. Therefore, a numerical process simulation for the introduced residual stresses was coupled with a fracture mechanics simulation [3]. To prove this approach for fuselage structures it is now transferred from a laboratory scale to larger

and thinner structures, here to M(T)200 specimens. Consequently, the next step was to apply this treatment on the state-of-the-art aerospace alloy AA2024 T3 with a thickness of 2 mm in a new experimental setup as well as to develop a new methodology to analyse its efficiency.

2 Experimental

2.1 Laser Heating Process

Process parameters like power, velocity and spot diameter were optimised to have a maximum effect on the residual stresses with minimal deterioration of the surface.

A typical airplane aluminium alloy, namely AA2024 T3 with a thickness of 2 mm, was used for the experiments. AA2024 is a common high-strength aluminium alloy. Typical uses are aircraft skins and structures [4].

Laser heating (LH) was performed using a 2.2-kW Nd:YAG laser with fibre optics (300-µm core diameter) and a 250-mm focal length. The laser was defocused in order to facilitate a bigger spot diameter on the specimen surface. The operating power was in the first case 300 W with a spot diameter of 2 mm and in the second case 600 W with a spot diameter of 3.5 mm on the specimen surface. The laser movement

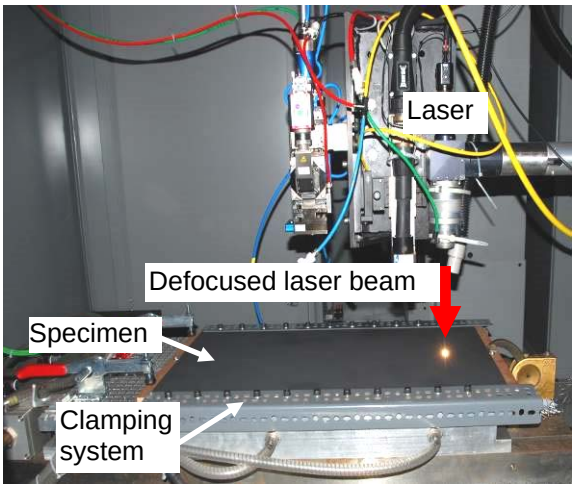

Fig. 1: Picture of the experimental setup for the laser heating treatment of AA2024 T3 sheets.

velocity was 1600 mm/min for both parameter sets. A black graphite layer was applied to the aluminium surface to reduce its reflectivity. A picture of the experimental setup is shown in Figure 1.

In order to carry out fatigue tests M(T)200 specimens were prepared out of the laser heat treated sheets. For symmetry reasons every specimen has two laser heating lines with a line distance of 80 mm to each other (see Fig. 2). The M(T)200 specimen is chosen because of its better comparability to the condition of a fatigue crack growth in an airplane structure in contrast to the formerly used C(T)100.

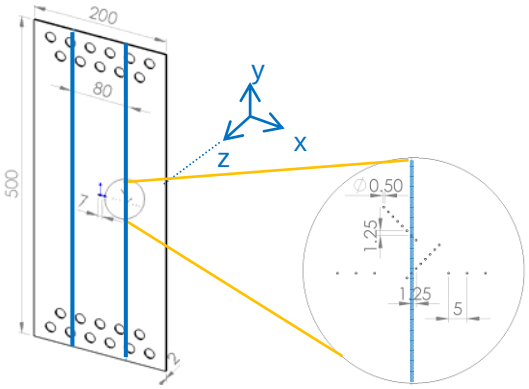

Fig. 2: Sketch of the investigated M(T)200 specimen. Marked in blue are the laser heating lines. Indicated as grey dots in the magnified area are the positions of the thermocouples.

2.2 Residual stress measurements

The residual stress measurement was performed at DESY (Deutsches Elektronen-Synchroton, Germany), beamline HEMS (High Energy Materials Science). The experimental setup is pictured in Figure 3 and described in detail in [2]. The residual stresses in x- and y- direction were measured in a transmission setup using a photon energy of 87 keV and a focussed beam which produced a spotsize of 0.5 x 0.5 mm on the sample surface.

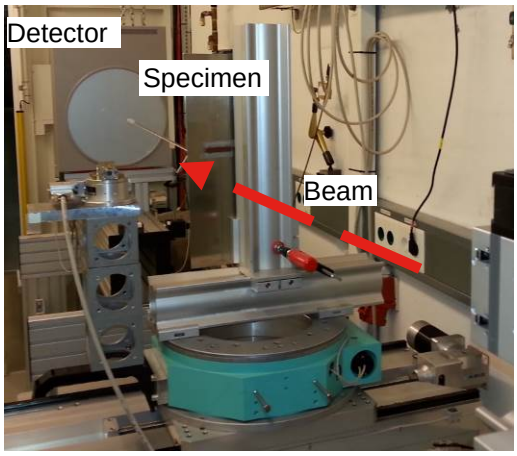

Fig. 3: Picture of the experimental setup for the residual stress measurement at DESY, Germany. Indicated by the red arrow is the direction of the x-ray beam. An area detector was used to determine the shift of the intensity maximum in x- and y- direction.

2.3 Hardness tests

In order to measure the changes of local mechanical properties which resulted from the laser heating, micro hardness measurements were carried out in series along the surface of the specimens. The device was equipped with a Vickers indenter tip. The applied load for each indent was 17.6 N (0.2 kp) with a holding time of 20 s.

2.4 Fatigue crack growth tests

For the investigation of the damage tolerance behaviour, the base material and the laser heated specimens were tested by constant amplitude fatigue crack growth (FCG) tests with a R-ratio of 0.1. The tests were performed with a servohydraulic testing machine (Schenck-Instron, 400 kN frame) at a frequency $f \approx 5$ Hz. The starter notches were created using an electro-discharging technique at a pre-determined location (see Figure 2). A notch of $2a_0 = 7$ mm was placed in the centre of the specimens between the laser heating lines. A pre-crack length of 10 mm was chosen as start of data evaluation. The crack direction was perpendicular to the laser heating lines. The crack length was measured optically using a travelling microscope.

3 Laser heating process simulation

The process simulation will be the key for the optimisation of the positioning of the laser heating lines in these structures. To determine the residual stress field a combined heat flux simulation and mechanical simulation has to be carried out, followed by a fracture mechanics simulation to predict the fatigue crack growth rate in dependence of the induced residual stresses [3]. ABAQUS was used for the whole finite element (FE) simulations. For symmetry reasons a half M(T)200 specimen was meshed and simulated to save calculation time.

The first step was the temperature field simulation. The heat flux density of the heat source was modelled as a Goldak ellipsoid volume heat source [5]:

$$Q(x,y,z,t) = Q_0 * \exp\left(-\frac{(y-y_0-v_y t)^2}{A^2} - \frac{(x-x_0)^2}{B^2} - \frac{(z-z_0)^2}{C^2}\right) \quad (1),$$

where Q_0 is the heat source amplitude, v_y is the travelling speed of the heat source in y-direction (see Fig. 2), A, B, C are the heat source shape parameters. x_0, y_0 and z_0 are the coordinates of the starting position for the laser heating. These values were gained by a fit of the thermal simulation to measurements of the local temperature during the laser heating with the help of several thermocouples positioned in holes in the centre of the sample. The positions of the thermocouples are illustrated in Figure 2 and all are in the middle of the plate at $z = 0$. For the applied laser power of 300 W, a heating parameter Q_0 of 15 W/mm^3, A and $B = 3$ mm and $C = 0.5$ mm were chosen. For the laser heating parameter of 600 W and spot diameter of 3.5 mm, a heating parameter Q_0 of 57 W/mm^3, A and $B = 2$ mm and $C = 0.5$ mm were chosen.

As thermal boundary conditions convection and radiation were assumed. The thermal emissivity is supposed to be 0.8 and the coefficient of convective thermal exchange is 25.0 W/(m^{2}K). A typical temperature field profile (here for 600 W laser power) during the laser heating process is shown in Figure 5.

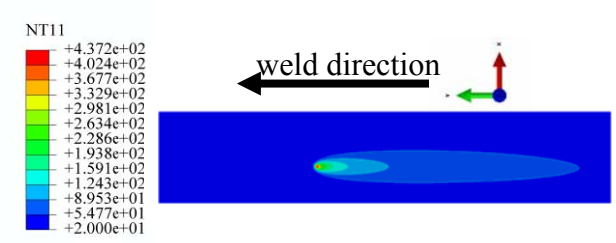

Fig. 4: Snap shot of local temperatures during a laser heating simulation (laser power 600 W) using a calibrated Goldak heat source.

4 Results and discussion

In order to validate the heat input and temperature profiles of the simulation, the local temperature in the specimen as a function of the distance to the heating line was measured by application of thermocouples over the whole specimen during the heating treatment. The maximum temperature for the laser heating parameters "300 W, 1600 mm/min, spot diameter 2 mm" was approximately 170 °C and fitted to the measured temperature profile in Figure 5a. The peak temperature for the laser heating parameters "600 W, 1600 mm/min, spot diameter 3.5 mm" was approximately 315 °C. The corresponding fit is shown in Figure 5b.

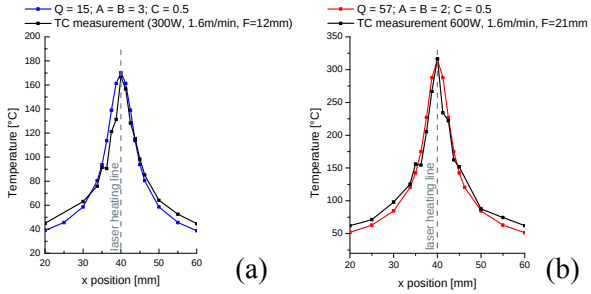

Fig. 5: Calibration of the Goldak heat source by comparison of the thermocouple (TC) measurements with the results of the thermal FE analysis for the (a) 300 W and (b) 600 W parameter set.

The resulting residual stress profiles as measured by x-ray diffraction are shown in Figure 6. The residual stress variation $\Delta\sigma$ is calculated by $\sigma_{YY} - \sigma_{XX}$. The measured stresses give an average through the whole specimen thickness because they were measured in a transmission setup. For the calculation of the stress components, the orientation distribution of the lattice distance from the stress-free condition and after laser heated treatment was used as described by Liu *et. al.* [6]. The determined transverse residual stresses σ_{XX} are as expected very small and the longitudinal residual stress variation $\Delta\sigma$ is dominated by σ_{YY}. In the case of the laser heating parameters for 300 W, tensile stresses of 125 MPa can be found in the heating line. In the vicinity of the heating line the corresponding compressive stresses are below the resolution limit of this method (Fig. 6). For the used laser heating parameters for 600 W, tensile stresses as high as 225 MPa were measured in the heating line. Compressive stresses neighbouring the tensile region of the heating line of -40 MPa developed during the heat treatment (Fig. 6).

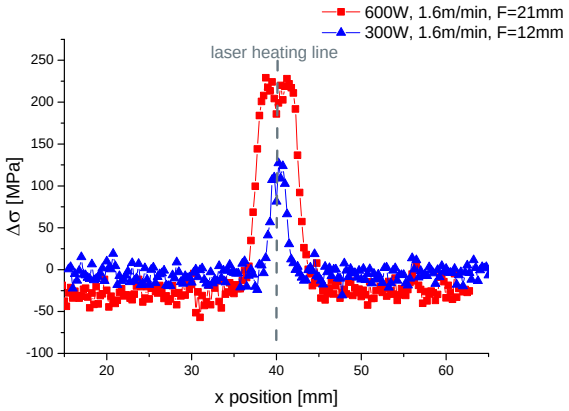

Fig. 6: Residual stress profile around the Laser Heating Line, measured at DESY

As a consequence of the high heat flux and high local temperature in the centre of the heating line, a small molten zone can be found on the laser heated surface. Figure 7 shows the cross sectional area of two specimens after laser heating treatment with 300 W (Fig. 7a) and 600 W (Fig. 7b). In the case of the low power treatment the molten zone is barely visible in opposite to the high power treatment where the molten zone goes up to several 100 µm into depth. The resolidified material on the upper part has distinctly coarser microstructure, the boundary to the unmolten material is clearly visible. This microstructural heterogeneity transfers to the local mechanical properties measured as microhardness over a cross section of a laser heated sample.

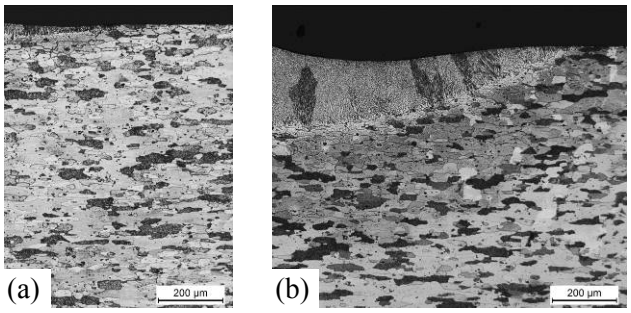

Fig. 7: Optical micrograph of the micro section of the laser heating line with parameters of (a) "300 W, 1600 mm/min, spot diameter 2 mm" and (b) "600 W, 1600 mm/min, spot diameter 3.5 mm".

The local distribution (Fig. 8) of determined hardness values shows a lower hardness in the area of the heating line in comparison to the base material in the outer region. Nevertheless, the laser heating causes only a small decline of the hardness which reaches through the whole sheet in the case of the high power treatment and effects only surface near regions in the case of the low power treatment.

The success in improvement of the damage tolerance of the investigated material by laser heating becomes visible by observation of the fatigue crack growth vs. the load cycles *N*. Figure 9 shows a comparison between heat treated and base material. There is a significant increase of the number of tolerated cycles of more than 10 %. Both sets of laser heating parameters show nearly the same increase in fatigue lifetime. The amount of molten surface obviously has no negative influence on the load cycles for the fatigue crack length. Interestingly, the different residual stress profiles of both parameters showed nearly the same increase of lifetime.

To retard the fatigue life time, the important stresses are the compressive residual stresses. For the compressive residual stresses in the lower power case of 300 W the resolution of the stress measurement was not high enough to quantify the modified stresses. For the parameter set for 600 W laser power, higher compressive residual stresses of 40 MPa near the heating line developed. There is no further increase in fatigue lifetime, despite the obviously higher compressive stresses.

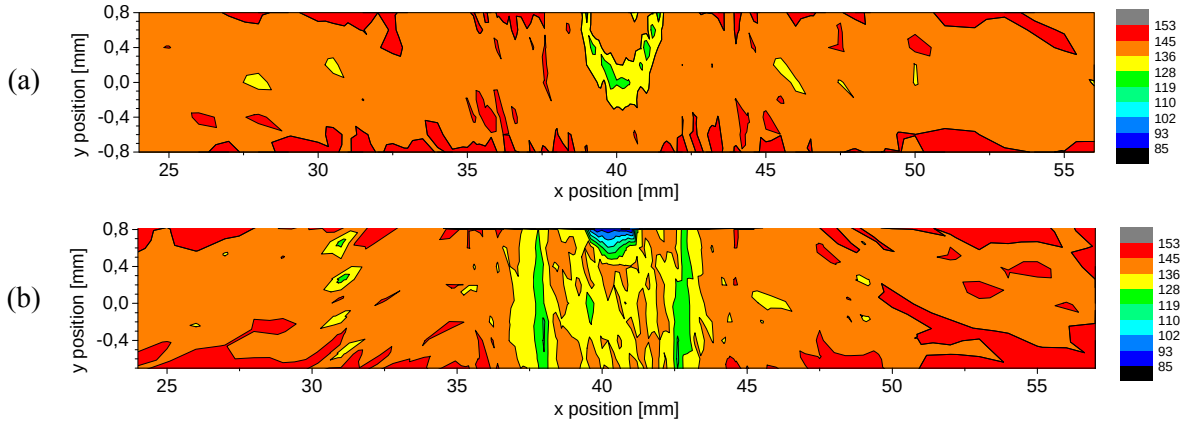

Fig. 8: Cross sectional distribution of Vickers hardness of the laser heated specimen (a) "300 W, 1600 mm/min, spot diameter 2 mm", (b) "600 W, 1600 mm/min, spot diameter 3.5 mm".

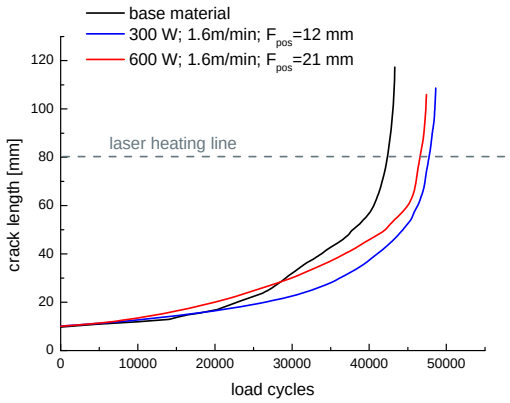

Fig. 9: Fatigue crack growth behaviour of the laser heated M(T)200 specimens at R-ratio 0.1 and the base material.

More relevant for technical purposes is the development of the fatigue crack growth rate. This can be easily derivated from the data in Figure 9 and is shown for the base material as well as the treated samples in Figure 10. The general trends of fatigue crack growth rate d*a*/d*N* vs. the load cycles *N* are identical to the development of the crack length vs. the load cycles *N*. When the propagating crack reaches the area of the heating line, a sudden retardation of the crack growth can be observed. After passing the heating line area the crack growth rate reaches its former value again. As a matter of course, this feature is missing in the corresponding curve of the base material.

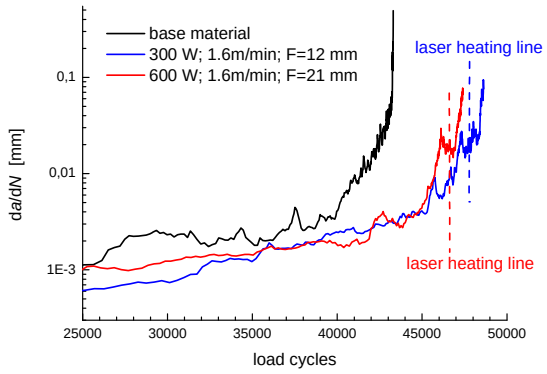

Fig. 10: Fatigue crack growth rate vs. the number of applied load cylces of the laser heated M(T)200 specimens at R-ratio 0.1 and the base material.

5 Conclusions

It is shown, that laser heating has significant influence on the fatigue life of aluminium AA2024 T3. We were able to achieve an increase of more than 10 % in fatigue life time for both tested laser parameter sets (power 300 W, velocity 1600 mm/min, spotsize 2 mm and power 600 W, velocity 1600 mm/min, spot diameter 3.5 mm). We conclude that using higher laser power probably will not lead to further increase in fatigue life. Here, more experiments are needed to evaluate the influence of scatter on the results. In additionally causes considerably more surface melting which might be unwanted during the production process. Different strategies like the application of multiple low power laser heating lines on different positions of the surface would promise higher impact on the efficiency of the presented method.

6 Acknowledgements

This work was carried out within the frame of the LISA project, which was supported by the research platform ACE of the division Materials Mechanics of the Helmholtz-Zentrum Geeesthacht. Parts of this research were carried out at the light source PETRA III at DESY, a member of the Helmholtz Association (HGF). We would like to thank Jie Liu, Peter Staron, René Kirchhof and Norbert Schell for assistance in using beamline HEMS. The authors also thank the following project members for their valuable work and support: Manfred Horstmann and Hamdi Tek (mechanical testing), René Dinse and Stefan Riekehr (laser heating experiments), and Falk Dorn (metallography).

7 References

[1] Masubuchi K. *Analysis of welded structures: residual stresses, distortion, and their consequences.* Pergamon Press, 1980.

[2] Schnubel D, Horstmann M, Ventzke V, Riekehr S, Staron P, Fischer T, Huber N. Retardation of fatigue crack growth in aircraft aluminium alloys via laser heating – experimental proof of concept. *Materials Science and Engineering* A 546(2012)8-14.

[3] Schnubel D, Huber N. Retardation of fatigue crack growth in aircraft aluminium alloys via laser heating – numerical prediction of fatigue crack growth. *Computational Materials Science*, Vol. 65, pp. 461-469, 2012.

[4] Starke Jr. E A, Staley J T. Application of modern aluminium alloy to aircraft. Pro 9. *Aerospace Sci.* Vol. 32, pp. 131-172, 1996.

[5] Radaj D. *Welding residual stresses and distortion: calculation and measurement.* DVS Verlag 2003.

[6] Liu J, Ventzke V, Staron P, Schell N, Kashaev N, Huber N. Investigation of in situ and conventional post-weld heat treatments on dual-laser-beam-welded γ-TiAl-Based Alloy. *Advanced Engineering Materials* 2012, 14, No.10, doi: 10.1002/adem.201200113.

8 Contact Author Email Address

anne.groth@hzg.de

Copyright Statement